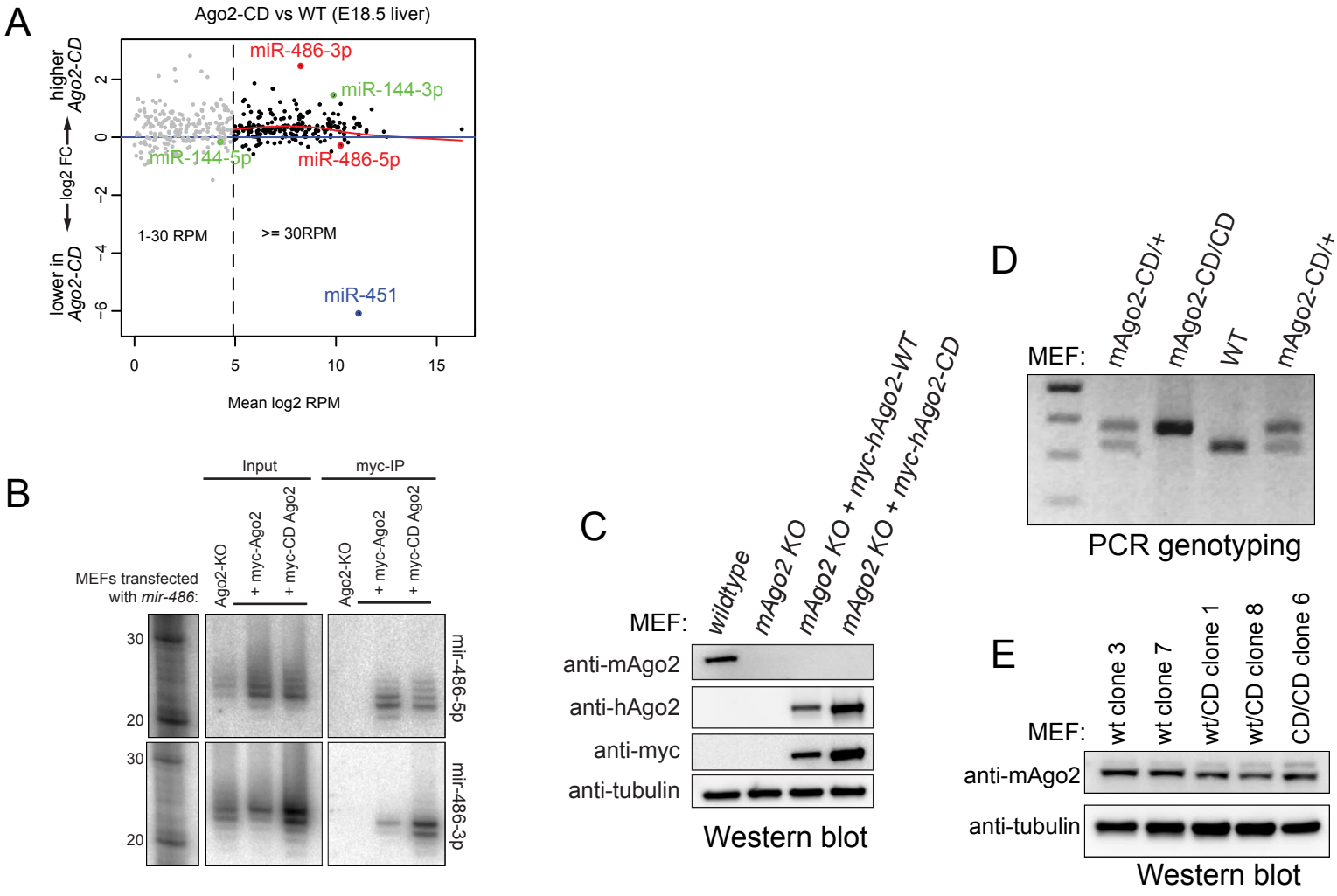

Figure S1. Expression pattern of *mir-451*/*mir-486* and validation of *Ago2-CD* MEFs, Related to Figure 1. **(A)** Re-analysis of total small RNA data from *wildtype* and *Ago2-CD* fetal liver (Cheloufi et al 2010). As reported, *mir-451* is strongly downregulated in *Ago2-CD* tissue. In addition, we observe strong selective increase in miR-486-3p (star strand) but not mature strand miR-486-5p. Most other miRNAs were not substantially affected. **(B)** miR-486-3p accumulates in the presence of catalytically dead (CD) Ago2. *Ago2-KO* MEFs, reconstituted with myc-hAgo2 or myc-hAgo2-CD, were transfected with *mir-486* expression construct and blotted for miR-486-5p and miR-486-3p. Input total RNAs are blotted on the left, and myc-IP RNAs are blotted on the right. miR-486-5p is modestly affected by Ago2 status, while miR-486-3p is reduced following reconstitution of Ago2, while it accumulates in the presence of hAgo2-CD. The increase in miR-486-3p is particularly evident in myc-Ago2 materials. **(C)** *Ago2-KO* MEF lines were reconstituted with myc-hAgo2-wt or myc-hAgo2-CD, and blotted for the indicated antibodies. **(D)** Genotyping for new MEF lines derived from *Ago2-CD* heterozygous and homozygous embryos. **(E)** Western blotting for *Ago2-CD* heterozygous and homozygous cell lines shows that they accumulate comparable levels of endogenous Ago2 as *wildtype* MEFs.

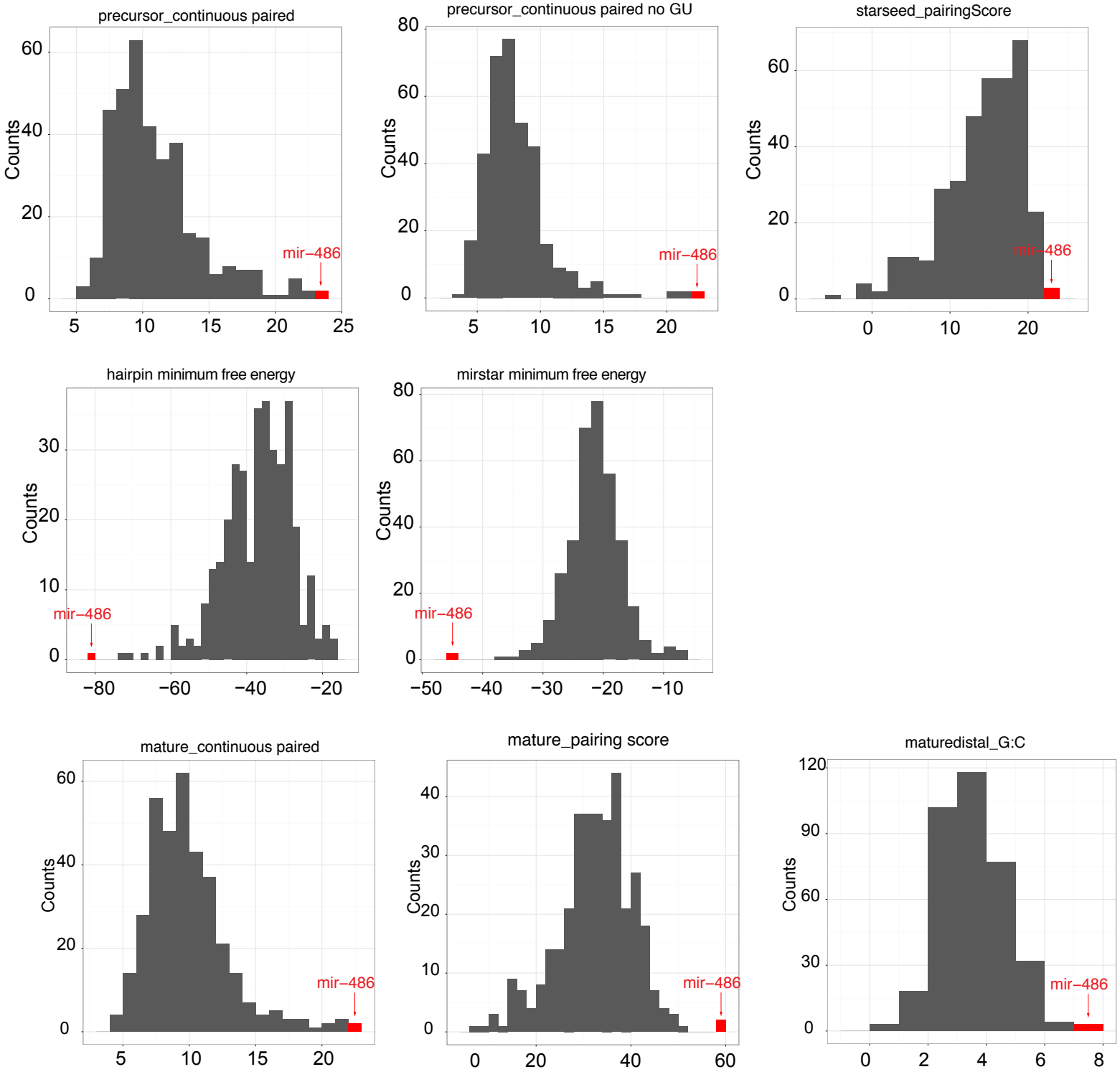

Figure S2. Distinctive structural and sequence features of mir-486, Related to Figure 4.
All conserved mammalian miRNAs were evaluated for a series of sequence features or structural features (GC content, continuous paired regions, pairing without GU, minimum free energy across different portions of the miRNA hairpin, etc.). *mir-486* is an outlier in essentially every single analysis, indicating that it has been evolutionarily selected for very atypical sequence and structural content.

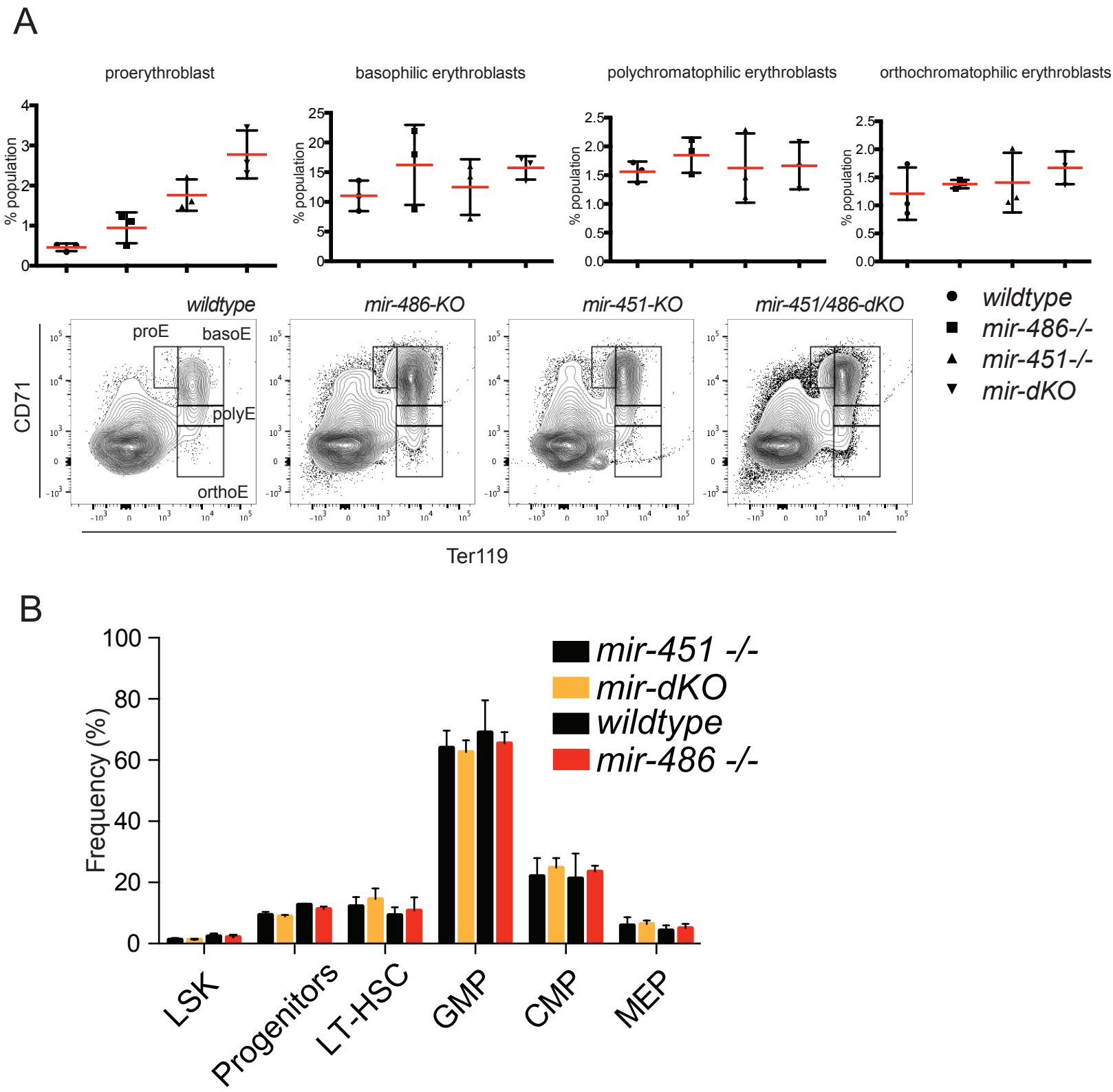

Figure S3. Bone marrow FACS analysis in miRNA mutants and controls, Related to Figure 6.
(A) FACS analysis of erythroid populations in the bone marrow of *wildtype*, *mir-486-KO*, *mir-451-KO*, and *mir-451/486-dKO* mice shows accumulation of the proerythroblast population in miRNA mutants. **(B)** Frequency of HSCs and progenitor populations in miRNA mutants and control mice.

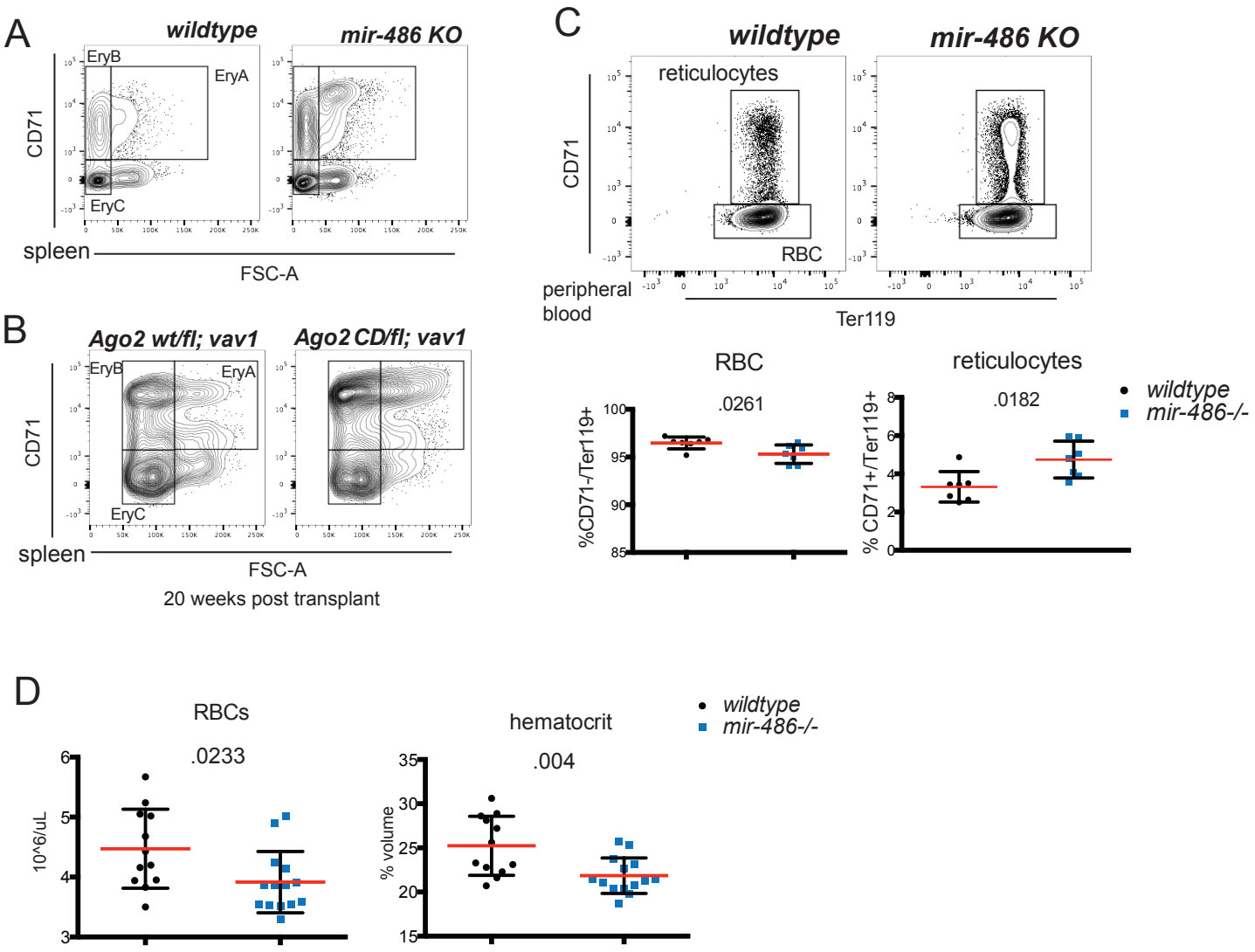

Figure S4. Additional erythroid phenotypes in *mir-486-KO* and *vav1>Ago2[fl/CD]* transplants, Related to Figure 6. (A) FACS analysis of erythroid progenitors in wildtype and *mir-486-KO* spleen. Quantified in Figure 6A. EryA/B accumulation and EryC reduction is observed in *mir-486-KO* mice. **(B)** Spleen FACS analysis in *vav1>Ago2[fl/CD]* transplant recipients and controls. Quantified in Figure 6F. EryA/B accumulation and EryC reduction is observed in *vav1>Ago2[fl/CD]* recipients. **(C)** Peripheral blood FACS analysis of *wildtype* and *mir-486-KO* mice at resting state reveals accumulation of immature reticulocytes and reduction in mature red blood cells in *mir-486-KO* mice. Corresponding data showing response of peripheral blood to hydrogen peroxide oxidative stress is shown in Figure 6B. **(D)** Peripheral blood counts of *wildtype* and *mir-486-KO* mice after treatment with phenylhydrazine shows greater reduction in red blood cell counts and volume in *mir-486-KO* mice.

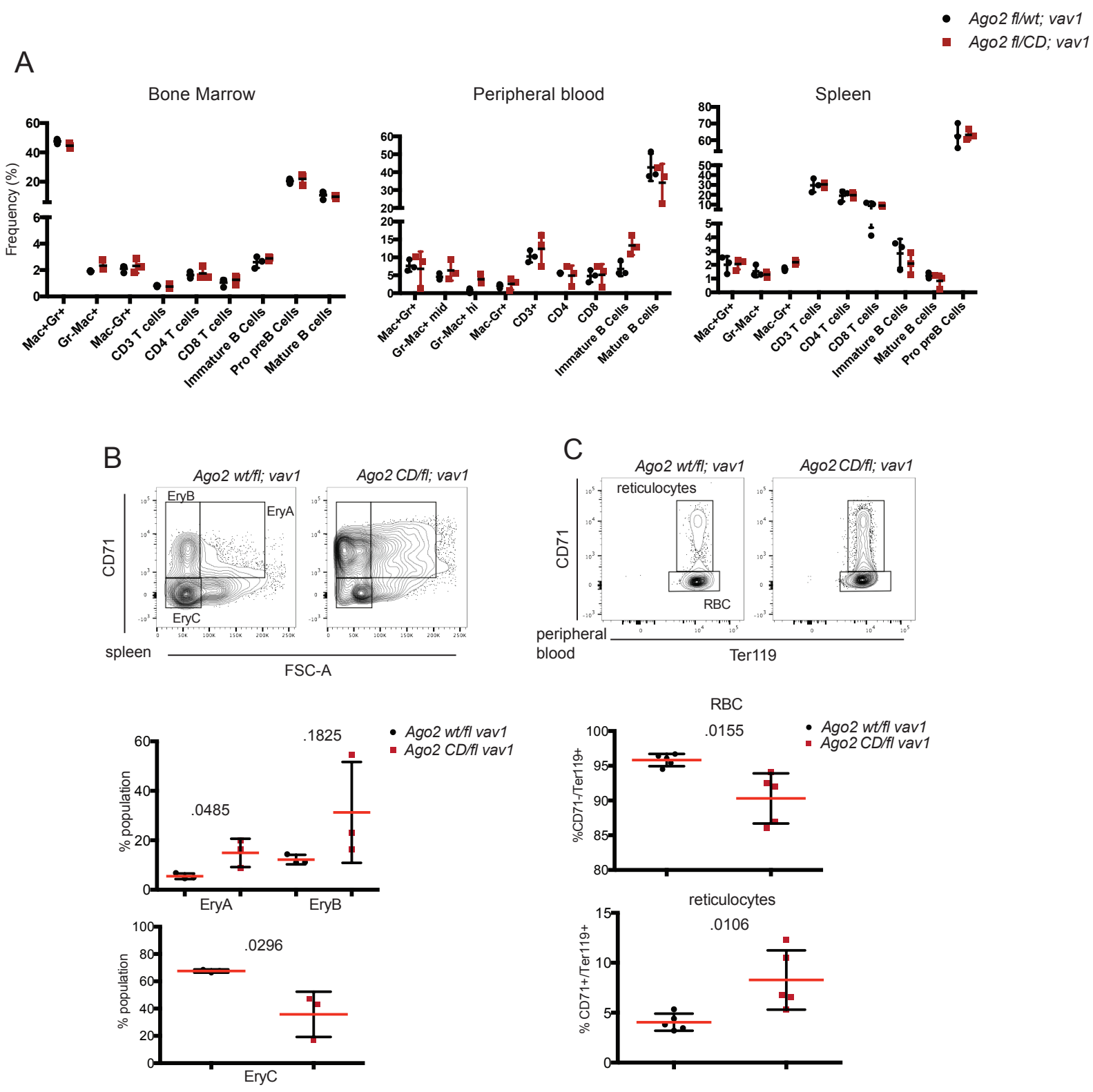

Figure S5. Analysis of hematopoietic populations in conditional Ago2 mutants and controls, related to Figure 6. (A) Analysis of various myeloid and lymphoid populations in conditional Ago2 mutants and controls shows no major difference outside of the erythroid lineage. **(B)** Accumulation of EryA erythroblasts and reductions in EryC cells is observed in the spleen of conditional Ago2 mutants. **(C)** Accumulation of immature reticulocytes in conditional Ago2 mutants.

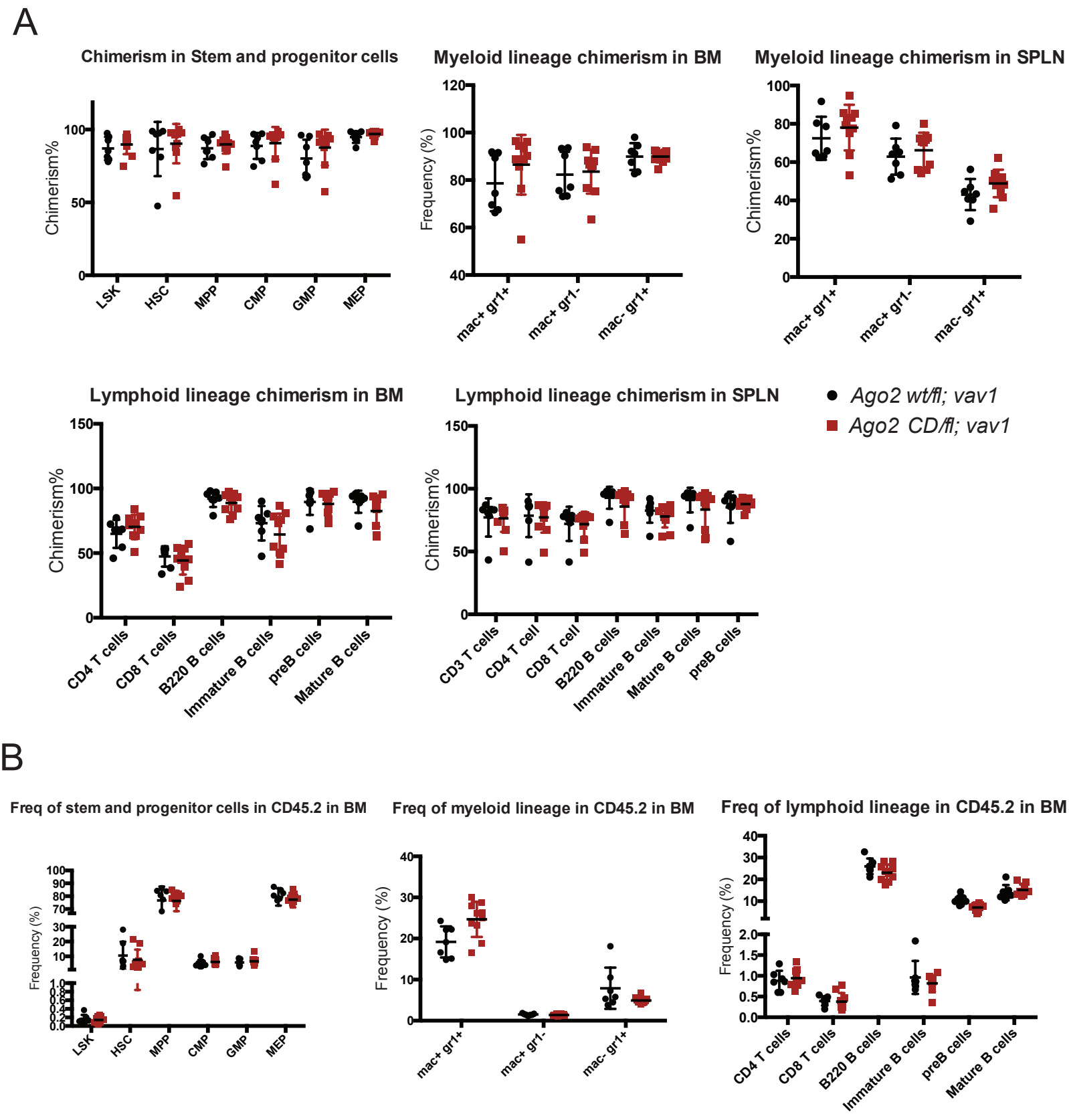

Figure S6. Transplant chimerism and profiling of hematopoietic populations in recipient mice, related to Figure 6. (A) Transplant chimerism percentage in stem, progenitor cells, and denoted populations measured in bone marrow and spleen. (B) Analysis of frequencies of various hematopoietic populations shows no major differences outside of the erythroid lineage.

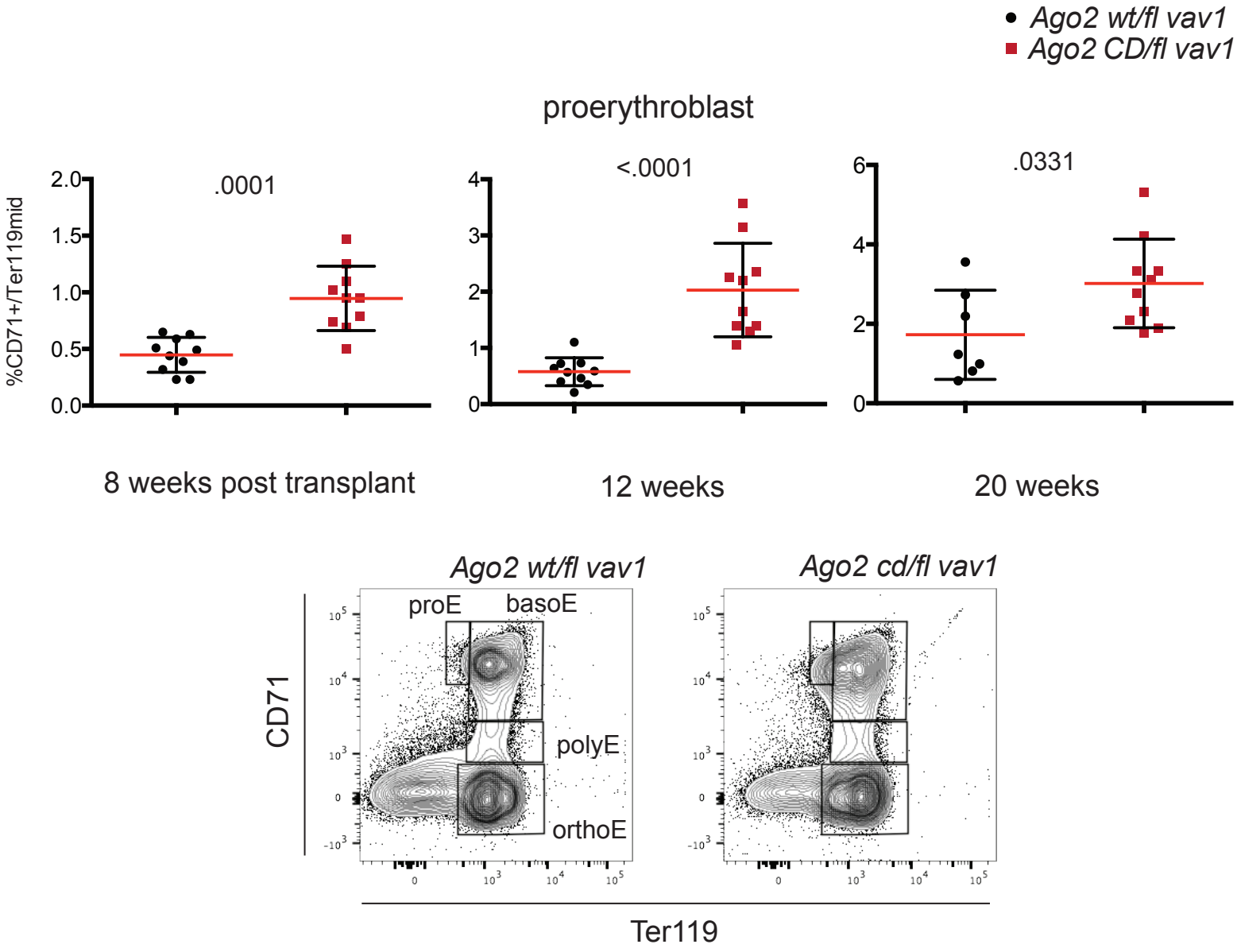

Figure S7. Erythroid phenotype in bone marrow of conditional Ago2 mutants, Related to Figure 6. Accumulation of proerythroblast population in *vav1>Ago2[fl/CD]* transplanted mice at all timepoints post transplantation (8 weeks, 12 weeks, and 20 weeks).